A HIF-1alpha-related gene involved in cell protection from hypoxia by suppression of mitochondrial function with transcriptional repression of mitochondrial transcription factor A

Yoshihiko Kakinuma, Rajesh G. Katare, Mikihiko Arikawa, *Kazuyo Muramoto, Fumiyasu Yamasaki, Takayuki Sato

Department of Cardiovascular Control, *Department of Physiology
Kochi Medical School, Nankoku, 783-85005, Japan

Running title: A HIF-1α-regulated gene suppresses energy metabolism in mitochondria

Corresponding author:

Yoshihiko Kakinuma, M.D., Ph.D.

Departement of Cardiovascular Control
Kochi Medical School
Nankoku, Kochi 783-8505
Japan

Tel: +81-(0)88-880-2587
Fax: +81-(0)88-880-2310
E-mail: kakinuma@kochi-u.ac.jp

Abbreviations: ACh, acetylcholine; HIF-1α, hypoxia-inducible factor-1α; UPR, unfolding protein response; ER, endoplasmic reticulum; VHL, von Hippel Lindau; AI, apoptosis inhibitor; WT, wild type; DN, dominant negative type; GFP, green fluorescence protein; siRNA, small interfering RNA; TFAM, mitochondrial transcription factor A; RCI, respiratory control index

Abstract

Recently, we reported that acetylcholine-induced HIF-1α protects cardiomyocytes from hypoxia; however, the downstream factors reducing hypoxic stress are unknown. We identified apoptosis inhibitor (AI) gene as being differentially expressed between von Hippel Lindau (VHL) protein-positive cells with high levels of GRP78 expression and VHL-negative cells with lower GRP levels, using cDNA subtraction. AI decreased GRP78 level, suppressed mitochondrial function, reduced oxygen consumption and, ultimately, suppressed hypoxia-induced apoptosis. By contrast, knockdown of the AI gene increased mitochondrial function. Hypoxic cardiomyocytes and ischemic myocardium showed increased AI mRNA expression. These findings suggest that AI is involved in suppressing mitochondrial function, thereby leading to cellular stress eradication and consequently to protection during hypoxia.

Keywords: hypoxia; transcription factor; cell protection; energy saving; gene

Introduction

To develop a novel therapeutic modality against heart failure, we extensively studied the cardioprotective effects of vagal nerve stimulation and the mechanisms underlying the anti-apoptotic actions of acetylcholine (ACh) [1]. Our previous study showed that induction of hypoxia-inducible factor (HIF)-1α is further activated by ACh in cardiomyocytes, even in normoxia. This additive induction of HIF-1α rescues cardiomyocytes from prolonged hypoxic stress and suppresses hypoxia-induced cell death [2]. These significant results prompted us to investigate which target genes are regulated by HIF-1α, and to reveal the mechanisms responsible for cardioprotection.

In order to escape from stresses, cells, including cardiomyocytes, possess self-defense systems, including HIF-1α induction against hypoxia, the unfolded protein response (UPR) against accumulated abnormal proteins, and the expression of heat shock proteins (Hsps) against heat shock [3-5]. Specifically, the stress induced by unfolded proteins in the endoplasmic reticulum (ER), ER stress, has been focused on as one of the causes of cardiovascular diseases, including cardiac hypertrophy and cardiac remodeling [6-8]. The ER plays crucial roles in protein folding and protein quality sensing, and is essential for cellular homeostasis. Therefore, ER stress is observed in situations where protein synthesis is augmented or cell proliferation is potentiated [9-11].

Among a variety of stresses, we have focused on a cardiac defense mechanism mediated by HIF-1α. The HIF-1α protein level is regulated by a proteasome system involving von Hippel Lindau (VHL) protein [12-15]. HIF-1α transcriptionally regulates target genes involved in glycolysis, angiogenesis and adaptation against hypoxic stress; therefore, HIF-1α induction might provide cells with fewer stresses, leading to escape from hypoxic stress. However, it remains unclear which factors are involved in the anti-stress effects induced by HIF-1α.

Recent studies have demonstrated that HIF-1α is induced through a nonhypoxic pathway mediated by cytokines, nitric oxide (NO) and ACh [2, 16]. These findings suggest that a cell defense system involving HIF-1α is modulated by molecules other than those involve in hypoxia. In order to elucidate the precise molecular mechanisms underlying the HIF-1α-regulated anti-stress effects, we compared VHL-negative and VHL-positive cells, that is, cells with higher and lower HIF-1α expression levels, respectively. We found that VHL-negative cells exhibited lower levels of ER stress. Using these cells, we subsequently performed a cDNA subtraction assay and identified a gene, apoptosis inhibitor (AI) gene, which may be involved in the anti-stress effects of

HIF-1α.

Materials and methods

Cell Culture

RCC4 cells, referred to as VHL-negative cells, and RCC4 cells with normal VHL expression, as VHL-positive cells, were generous gifts from Dr. Patrick H. Maxwell (The Wellcome Trust Center for Human Genetics, Oxford, UK) [15]. They were cultured in DMEM containing 10% FBS and 1 mg/ml G418. Primary cardiomyocytes isolated from neonatal rats and H9c2 cells derived from rat ventricular myocytes were also used. HEK293 (human embryonic kidney) cells, cultured in DMEM containing 10% FBS, were used for transfections, since the transfection efficiency was better.

cDNA Subtraction Assay

In order to screen for genes that were more highly expressed in VHL-negative cells than in VHL-positive cells, a cDNA subtraction assay was performed using a SMART^{TM} PCR cDNA Synthesis Kit and a PCR-Select^{TM} cDNA Subtraction Kit (CLONTECH Laboratories Inc., Palo Alto, CA, USA) [17], as previously described [2]. The results of the subtraction assay were then evaluated by RT-PCR using nested primers targeting the sequenced genes. After searching the database using a segment of an interesting gene, the full-length sequences of interesting genes were obtained from GenBank; and those full-length genes were subcloned into pcDNA3.1 expression vector with a His tag sequence, or pIRES-EGFP (Clontech, Mountain View, CA, USA).

Western Blot Analysis

Whole cell lysates from VHL-positive or VHL-negative cells were fractionated by SDS-PAGE and transferred onto membranes (Millipore Corp., Bedford, MA, USA). The membranes were incubated with antibodies against GRP78, HIF-1α, VHL (BD Biosciences, San Jose, CA, USA) or α-tubulin. After reaction with secondary antibodies, the signals were detected using ECL Plus (Amersham, Buckinghamshire, UK).

Transfection of HEK293 Cells

The AI gene was transfected into HEK293 cells using Effectene^{TM} (QIAGEN, Valencia, CA, USA). In gene knockdown experiments, siFECTOR^{TM} (B-Bridge International, Inc., Sunnyvale, CA, USA) was used. In another experiment for transfection, wild-type (WT) or dominant negative (DN) HIF-1α vector, subcloned into pcDNA3.1 expression vector, was also used [2]. Forty eight hours after transfection, the cells were used for further studies.

Reporter Assay for Mitochondrial Transcription Factor A (TFAM) Transcriptional Activity

The 5'-regulatory promoter region of rat TFAM (700 bp) was subcloned into a reporter vector (TOYO B-Net Co. Ltd., Tokyo, Japan) [18]. The reporter vector was co-transfected with or without the AI gene expression vector into HEK293 cells. Forty eight hours later, the cells were lysed and the luciferase activities were measured and corrected by the levels produced by the SeaPansy luciferase vector (TOYO B-Net Co. Ltd., Tokyo, Japan).

RT-PCR

Total RNA was isolated from VHL-negative and VHL-positive cells and reverse-transcribed to obtain first-strand cDNAs, which was amplified using specific primers for the AI gene, as follows: AI (sense), 5'GAATGCAGAAAAGCTTCATG3'; AI (antisense), 5'TAGCTAGCTCAGTAGAGTCTTTCCCC3'. PCR products were fractionated by electrophoresis.

Assessment of Cell Number

After performing MTT reduction assays, the cells were treated with a 0.05% trypsin-0.23 mM EDTA solution. And the cell number of the suspension was counted.

MTT Activity Assay

Measurements of 3-(4,5-dimethylthiazol-2-yl)-2,5-diphenyl tetrazolium bromide (MTT) reduction activity were performed in cells, which were transfected with or without the AI gene, containing comparable cell numbers, using an assay kit (Dojindo, Kumamoto, Japan). The mitochondrial function of cardiomyocytes was also evaluated using this assay system [19].

Caspase-3 Activity Assay

Caspase-3 activity was measured using an assay kit (MBL, Tokyo, Japan) [20]. Briefly, cell lysates were mixed with a caspase-3 substrate and fluorometric measurements were performed. The caspase-3 activity in hypoxic cells was compared with that in normoxia.

Flow Cytometry Analysis

HEK293 cells were cotransfected with GFP and AI genes, or transfected with the GFP gene alone, and then analyzed by flow cytometry to examine whether the AI gene affected the cell cycle. After suspended cells were fixed in 70% ethanol, they were

treated with RNAase A (1 mg/mL) and mixed with propidium iodide (20 mg/mL); cells were then analyzed using a FACSCalibur System (Becton Dickinson, Boston, USA). The percentage of each cell cycle phase was compared.

Immunocytochemistry of Transfected cells

Localization of the AI protein was analyzed by immunocytochemistry. Transfected HEK293 cells were fixed and treated with 0.1% Triton X100. After blocking, cells were incubated with an anti-His monoclonal antibody (QIAGEN, Valencia, CA, USA), followed by incubation with an FITC-conjugated anti-mouse IgG antibody, and finally analyzed by fluorescence microscopy.

Adenoviral Infection of the AI Gene into Rat Primary Cardiomyocytes

The full-length human AI gene was subcloned into the pShuttle vector possessing CMV promoter according to the protocol. As a negative control, pShuttle vector containing LacZ was also prepared. After linearization, the plasmids were each co-transfected into *Escherichia coli* together with pAd, an adenoviral DNA plasmid (BD Adeno-X Expression System, BD Biosciences, San Jose, CA, USA). Recombinant adenoviral constructs were selected, digested with PacI and transfected into HEK293 cells to produce viral particles. Adenoviral infection was performed at a multiplicity of infection (MOI) of 100. Rat cardiomyocytes were transfected with the adenovirus for 72 hours and used for further experiments.

Analysis of the Intracellular Calcium Response in AI-transfected Cells

pIRES-EGFP expression vector containing the AI gene was transfected into HEK293 cells. After 48 hours, these cells were loaded with a rhod-2 AM ester (5 μM; Molecular Probe, Eugene, OR, USA), and then stimulated with 100 μM ACh, which phosphorylates Akt through muscarinic receptors. The calcium responses in AI-expressing cells were evaluated using an imaging system (AQUACOSMOS, Hamamatsu Photonics, Hamamatsu, Japan) and analyzing software.

Measurement of Oxygen Consumption by Cells

At 48 hours after transfection, cells were lysed in a lysis buffer, and the mitochondrial fraction was obtained by sequential centrifugation. Pellets were resuspended in a suspension buffer, and mitochondrial respiration was initiated by the addition of 30 mM ADP, 1.2 M succinate and 0.5 M PBS. The mixture was applied to a Biological Oxygen Monitor (YSI Japan Ltd., Tokyo, Japan) and the respiratory control index (RCI) was

evaluated as the ratio of state 3 to state 4 respiration.

siRNA for AI

To silence the effect of AI gene expression in HEK293 cells, small interfering RNAs (siRNAs) were used. The best sequence of siRNA duplex was selected, and an siRNA duplex of 21-nucleotides was synthesized (TAKARA BIO INC., Otsu, Japan). The sense strand of the siRNA for the AI gene (AI siRNA) was GAACAAUGCCCUAUUAAGUTT. Nonspecific siRNA was also used as a negative control for comparison (CCGUUUACAACGAUAGAAUTT, unrelated siRNA). Transfection was carried out using siFECTOR (B-Bridge International, Inc., Sunnyvale, CA, USA) with 50 pmol/dish siRNA added to 1.5 μl of siFECTOR according to the manufacturer's protocol.

Statistical Analysis

The data are presented as means ± S.E. Mean values were compared between the two groups using an unpaired Student's t-test. Differences among data from the in vitro studies were assessed by ANOVA for multiple comparisons of results. Differences were considered significant at $P<0.05$.

Results

VHL-negative Cells Express More HIF-1α but Less GRP78 than VHL-positive Cells under Normoxia with a Decrease in Mitochondrial Function

As shown in Figure 1, the HIF-1α protein level was higher in VHL-negative cells than VHL-positive cells. By contrast, the VHL protein level was decreased in the former cells, indicating that the HIF-1α protein expression level is increased in VHL-negative cells, even under normoxia.

As shown in Figure 2A, neither of the cell types showed any cell death, regardless of the VHL expression level, as evaluated by the absence of floating cells. Both cell types comparably reached 100% confluence. To investigate the other characteristic differences between them, the expression levels of GRP78, an ER stress marker, were examined. VHL-negative cells showed lower GRP78 expression levels than VHL-positive cells, indicating that the former cells are subjected to less ER stress (Figure 2B). Furthermore, MTT reduction activity was lower in VHL-negative cells (74.6±5.3%) than VHL-positive cells (100.0±3.7%; n=6, $P<0.01$), despite the comparable cell numbers (Figure 2C). This result indicates that the mitochondrial function in VHL-negative cells is relatively decreased, because MTT reduction activity depends on mitochondrial respiratory chain function.

cDNA Subtraction to Identify Genes Responsible for the Lower Expression of GRP78

VHL-negative cells, with a high HIF-1α level under normoxia, showed a decreased GRP78 expression in response to stress. Therefore, we hypothesized that VHL-negative cells show less stress than VHL-positive cells, and that some HIF-1α-regulated genes, which modulate the stress level, could be identified by screening via cDNA subtraction between two cell types. Thereafter, we obtained one gene, which had already been reported, with the GenBank accession number (BT008120) and tentatively named apoptosis inhibitor (AI) 5 gene. As depicted in Figure 3A, the AI mRNA level was increased in VHL-negative cells compared with VHL-positive cells. The AI mRNA expression levels were increased by hypoxia (1% oxygen) in both HEK293 and H9c2 cells (Figure 3B), suggesting that AI expression is induced by hypoxia. Analysis of the tentative 5'-promoter region of the AI gene in the EMBL database revealed one hypoxia-responsive element (HRE), a DNA-binding site for HIF-1α, in that region (AY265937). This finding may support our results.

HIF-1α increases AI mRNA levels and negatively affects GRP78 expression

To confirm that HIF-1α directly affects AI gene expression and, furthermore, GRP78 expression, the effects of wild-type (WT) HIF-1α on the expression of AI gene were compared with those of dominant negative (DN) HIF-1α. AI mRNA expression was decreased by DN HIF-1α, compared with WT HIF-1α (69.3±0.8% vs. 175.3±11.8%, n=6, $P<0.01$) (Figure 3C). By contrast, DN HIF-1α adversely increased the GRP78 expression level, compared with WT HIF-1α (190.9±2.7% vs. 114.4±2.7%, n=3, $P<0.05$). The difference in the effects of WT and DN HIF-1α on AI mRNA or GRP78 expression was more evident than between those of control and WT HIF-1α. These findings suggest that HIF-1α positively regulates AI gene expression and also affects GRP78 expression (Figure 3D).

Nuclear AI is Involved in the Reduced GRP78 Expression

To investigate the function of the AI gene, the GRP78 response was assessed in the presence of tunicamycin, an ER stressor. In the presence of tunicamycin, the GRP78 expression levels were increased in non-transfected control cells, GFP-transfected cells and empty expression vector-transfected cells. However, compared with these cells showing increased GRP78 levels, AI-transfected cells exhibited remarkably decreased GRP78 expression (Figure 3E). Using an anti-His-tag antibody, AI was detected in the nucleus (Figure 3F). However, the proportions of cells at each cell cycle phase were comparable between the AI-transfected cells and non-transfected cells (55.0% and 58.6% in G1 phase, 28.8% and 25.9% in S phase, and 16.3% and 15.4% in G2+M, respectively) (data not shown), suggesting that AI does not affect the cell cycle.

AI Modifies Mitochondrial Function through Downregulation of TFAM

Despite the presence of comparable cell numbers, as shown in Figure 4A, MTT reduction activity was decreased in AI-transfected cells (to 43.0±2.5%) compared with GFP-transfected cells (101±3.1%; n=8, $P<0.01$), indicating that AI inhibits mitochondrial function, as occurs in VHL-negative cells (Figure 2C), since the MTT reduction activity reflects complex II activity in mitochondria. To investigate the mechanism by which mitochondrial function is affected by AI, reporter assays were carried out using a 5'-flanking regulatory region of the human mitochondrial transcriptional factor A (TFAM) gene. TFAM is an essential transcription factor encoded by nuclear DNA, which regulates the transcription of mitochondrial DNA. The transcriptional activity of the reporter vector in the presence of the TFAM flanking region (TFAM) was 378±15 or 739±55 RLU compared with the basic vector or SV promoter vector alone, respectively (Figure 4B). By contrast, AI decreased the

luciferase activity (TFAM+AI) to 267±10 or 397±019 RLU, respectively, suggesting that AI interferes with TFAM transcriptional activation (n=8, P<0.01 vs. TFAM), and inhibits mitochondrial function.

AI Attenuates Calcium Response Following Stimulation

The facts that AI reduces GRP78 expression, TFAM transcription and mitochondrial function prompted us to speculate that AI suppresses various cellular responses, including the calcium response. Therefore, we investigated the effect of AI on the calcium response. It had already been confirmed that ACh phosphorylates Akt and modulates intracellular calcium levels in HEK293 cells (data not shown). Intracellular calcium levels were elevated in GFP-transfected cells stimulated by ACh (100 μM) (upper panel in Figure 4C). This elevation was comparable with the calcium responses seen in non-transfected HEK293 cells (data not shown). However, as shown in the lower panel, the calcium responses in AI-transfected cells were remarkably attenuated, suggesting that AI affects the calcium response (n=20, P<0.05 vs. GFP).

AI Gene Decreases Oxygen Consumption in Cardiomyocytes

Oxygen consumption was evaluated using the respiratory control index (RCI) (Figure 4D). In AI-transfected HEK293 cells, the RCI was decreased (to 1.3±0.1), compared with that in GFP-transfected cells (2.0±0.1; n=5, P<0.05). Likewise, adenoviral infection of AI into rat primary cardiomyocytes caused a decrease in RCI (to 1.5±0.1), compared with that in LacZ-transfected cells (2.0±0.1; n=5, p<0.05). These results indicate that AI decreases oxygen consumption and leads to a decrease in energy metabolism.

AI Decreases the Hypoxia-induced Elevation of Caspase-3.

In the absence of the AI gene, hypoxia (1% oxygen) increased caspase-3 activity (to 128.0±3.0%). By contrast, hypoxia did not increase caspase-3 activity in AI-transfected HEK293 cells (89.5±1.4%; n=5, P<0.01) (Figure 4E), suggesting that AI inhibits the apoptosis induced by hypoxia. AI was identified to suppress mitochondrial function, therefore, it could be speculated that AI is induced by an adaptation to hypoxia. Inadequate induction level of AI can not efficiently prevent hypoxia-induced apoptosis; however, greater levels of AI induction could lead to cellular protection.

Knockdown of AI using siRNA increases MTT reaction activity even with comparable cell numbers

To clarify the significance of AI, AI siRNA or unrelated siRNA was transfected into HEK293 cells. Initially, the efficiency of siRNA to knockdown AI expression was verified (Figure 4F). AI expression, detected in the nucleus, was greatly suppressed by the AI siRNA. Compared with the MTT reduction activities in non-transfected cells (control, 100±6.3%) or unrelated siRNA-transfected cells (unrelated siRNA, 98.7±5.1%), the MTT activities of AI siRNA-transfected cells were significantly higher, even with adjustment for cell numbers (AI siRNA, 150.0±6.0%; $n=10$, $p<0.01$ vs. control and unrelated siRNA). Taken together with the results from the AI gene introduction study, this finding suggests that AI plays a pivotal role in regulating mitochondrial function.

Acute myocardial ischemia increases AI mRNA

Ischemia of the heart, induced by left coronary ligation for 3 hours, resulted in an increase in AI mRNA expression (Figure 4G), consistent with an earlier finding in H9c2 cells, which showed increased AI mRNA expression in response to hypoxic stress (Figure 3B). This in vivo result suggests that AI induction by ischemia may be due to adaptation of the heart.

Discussion

The present study revealed that AI exerts anti-stress effects by suppressing mitochondrial function, thereby reducing oxygen consumption and inhibiting hypoxia-induced apoptosis. These effects are achieved via transcriptional repression of mitochondrial transcription factor A (TFAM). This study, therefore, shows that AI plays a crucial role in suppressing mitochondria during hypoxia, leading to the salvaging of cells.

These results suggest a potential advantage of a nonhypoxic induction pathway of HIF-1α in a clinical setting. We have recently revealed that ACh exerts a cardioprotective action through the PI3K/Akt/HIF-1α/VEGF signaling pathway, and that it inhibits the collapse of mitochondria membrane potential [2]. Therefore, the possibility is raised that the beneficial effects of ACh might be attributed to modulation of cardiac mitochondria. However, there are few adequate studies regarding the linkage between ACh and mitochondrial function in cardiomyocytes. Therefore, we have studied which factors might link HIF-1α to mitochondrial function and then found a cue from AI gene.

TFAM plays key roles in mitochondrial DNA maintenance and mitochondrial biogenesis, since complete inactivation of TFAM causes cardiomyopathy [21, 22]. Therefore, TFAM is definitely essential for the homeostasis of energy metabolism in cells. In the present study, however, AI partially decreased the TFAM promoter activity and suppressed oxygen consumption. It was therefore revealed that the principal function of AI is to decrease energy metabolism, and that AI plays a role in protecting cells against hypoxia. Since AI is screened from cells with higher expression levels of HIF-1α, these results are compatible, and suggest that AI is one of the targets of HIF-1α responsible for cell protection against hypoxic conditions.

The AI gene has already been reported under GenBank accession number BT008120 as an apoptosis inhibitor (AI). One study reported another related gene, designated the AAC-11 gene, which shows partial amino acid sequence identity to the AI gene [23]. AAC-11 gene-transfected cells are resistant to apoptosis [23, 24]; just as AI-transfected cells are resistant to hypoxia-induced apoptosis. It was demonstrated that increased AAC-11 mRNA expression is correlated with a poor prognosis for patient with non-small cell carcinoma [24] and cervical carcinoma [25]. Unlike AAC-11, however, the functions of BT008120, AI, have remained unknown. Therefore, our present study reveals a novel function of AI in terms of the modification of mitochondrial function.

Based on the facts that VHL-negative cells with higher HIF-1α expression levels

showed lower MTT reduction activity than VHL-positive cells, it is suggested that VHL-negative cells utilize less mitochondrial function, because the MTT reduction activity represented by complex II activity is reduced. It is further suggested that increased HIF-1α expression is adversely related to decreased mitochondrial function. Compatible with this, the levels of AI mRNA were increased by hypoxia and ischemia, and AI gene expression was increased by HIF-1α.

Cardiomyocytes, which are rich in mitochondria, efficiently produce adequate ATP through the mitochondrial respiratory chains, but simultaneously produce endogenous reactive oxygen species (ROS). It was also established that mitochondria play crucial roles in executing apoptosis [26, 27]; therefore, β-blockers are widely used in patients with heart failure to achieve a better outcome [28-32] through the reduction of cardiac work, as AI suppresses mitochondrial energy metabolism via a decrease in oxygen consumption. Consequently, it is suggested that AI suppresses energy metabolism, resulting in the circumvention of apoptotic stresses.

In agreement with this, AI also decreased the level of GRP78 expression, suggesting that AI reduces cellular stress, decreases caspase-3 activity induced by hypoxia and attenuates the calcium response. The UPR is activated by stresses and up-regulates protective ER-related proteins, including GRP78. Recent studies have revealed that hypoxia causes ER stress in cardiomyocytes with elevated GRP78 levels [33, 34]. According to an elegant study by Terai et al. [34], activation of a cell-protective kinase (AMPK) inhibits apoptosis without GRP78 induction. A crucial point in our present study is that AI also exerts cell-protective effects upstream of GRP78, and primarily makes cells more resistant to stress by suppressing energy metabolism. It is therefore speculated that a reduction of energy metabolism by AI is associated with the diminution of oxidative stresses, lower proliferation and decreased protein synthesis, and that these mechanisms could decrease ER stress [35]. Consequently, this study reveals a missing link between AI, HIF-1α, mitochondria and stresses.

Although AI decreased MTT reduction activity in normoxia, leading to decreased mitochondrial function, MTT reduction activity was surprisingly up-regulated by knockdown of AI, indicating that mitochondrial function is adversely activated by AI siRNA. Taken together, these findings suggest that AI plays a critical role in negatively modulating mitochondrial function.

In conclusion, the present study has identified the AI gene, which is regulated by HIF-1α, as a candidate gene that may be involved in the inhibition of energy metabolism and apoptosis under hypoxic conditions. These effects of AI could contribute to cellular protection.

Acknowledgements

We would especially like to thank to Dr. M. Miura, Dr. M. Kuroda, S. Kataoka, and K. Yokota for technical advice and significant discussions. This work was supported by Grants-in-Aid from the Japan Society for the Promotion of Science (19590251). It was also supported in part by a Health and Labor Sciences Research Grant (H15-PHYSI-001) for Advanced Medical Technology from the Ministry of Health, Labor, and Welfare of Japan.

References

1. Li, M., Zheng, C., Sato, T., Kawada, T., Sugimachi, M., and Sunagawa, K. (2004). Vagal nerve stimulation markedly improves long-term survival after chronic heart failure in rats. *Circulation* 109,120-124.
2. Kakinuma, Y., Ando, M., Kuwabara, M., Katare, G.R., Okudela, K., Kobayashi, M., and Sato T. (2005). Acetylcholine from vagal stimulation protects cardiomyocytes against ischemia and hypoxia involving additive non-hypoxic induction of HIF-1alpha. *FEBS Lett.* 579, 2111-2118.
3. Semenza, G.L. (2001). HIF-1, O(2), and the 3 PHDs: how animal cells signal hypoxia to the nucleus. *Cell* 107, 1-3.
4. Rutkowski, D.T., Kaufman, R.J. (2004). A trip to the ER: coping with stress. *Trends Cell Biol.* 14, 20-28.
5. Latchman, D.S. (2000). Heat shock proteins and cardiac protection. *Cardiovasc Res.* 51, 637-646.
6. Okada, K., Minamino, T., Tsukamoto, Y., Liao, Y., Tsukamoto, O., Takashima, S., Hirata, A., Fujita, M., Nagamachi, Y., Nakatani, T., Yutani, C., Ozawa, K., Ogawa, S., Tomoike, H., Hori, M., and Kitakaze, M. (2004). Prolonged endoplasmic reticulum stress in hypertrophic and failing heart after aortic constriction: possible contribution of endoplasmic reticulum stress to cardiac myocyte apoptosis. *Circulation* 110, 705-712.
7. Hamada, H., Suzuki, M., Yuasa, S., Mimura, N., Shinozuka, N., Takada, Y., Suzuki, M., Nishino, T., Nakaya, H., Koseki, H., and Aoe, T (2004). Dilated cardiomyopathy caused by aberrant endoplasmic reticulum quality control in mutant KDEL receptor transgenic mice. *Mol Cell Biol.* 24, 8007-8017.
8. Kostin, S., Pool, L., Elsasser, A., Hein, S., Drexler, H.C., Arnon, E., Hayakawa, E., Zimmermann, R., Bauer, E., Klovekorn, W.P., and Schaper, J. (2003). Myocytes die by multiple mechanisms in failing human hearts. *Circ Res.* 92, 715-724.
9. Verkhratsky, A., and Toescu, E.C. (2003). Endoplasmic reticulum Ca(2+) homeostasis and neuronal death. *J Cell Mol Med.* 7, 351-361.
10. Forman, M.S., Lee, V.M., and Trojanowski, J.Q. (2003). 'Unfolding' pathways in neurodegenerative disease. *Trends Neurosci.* 26, 407-410.
11. Hampton, R.Y. (2002). ER-associated degradation in protein quality control and cellular regulation. *Curr Opin Cell Biol.* 14, 476-482.
12. Minet, E., Michel, G., Mottet, D., Raes, M., and Michels, C. (2001). Transduction pathway involved in hypoxia-inducible factor-1 phosphorylation and activation.

Free Radical Biol Med. 31, 847-855.

13. Maxwell, P.H., Wiesener, M.S., Chang, G.W., Clifford, S.C., Vaux, E.C., Cockman, M.E., Wykoff, C.C., Pugh, C.W., Maher, E.R., and Ratcliffe, P.J. (1999). The tumour suppressor protein VHL targets hypoxia-inducible factors for oxygen-dependent proteolysis. *Nature* 399, 271-275.
14. Min, J.H., Yang, H., Ivan, M., Gertler, F., Kaelin, W.G. Jr, Pavletich, N.P. (2000). Structure of an HIF-1alpha -pVHL complex: hydroxyproline recognition in signaling. *Science* 296, 1886-1989.
15. Cockman, M.E., Masson, N., Mole, D.R., Jaakkola, P., Chang, G.W., Clifford, S.C., Maher, E.R., Pugh, C.W., Ratcliffe, P.J., Maxwell, P.H.(2000). Hypoxia inducible factor-alpha binding and ubiquitylation by the von Hippel-Lindau tumor suppressor protein. *J Biol Chem* 275, 25733-25741.
16. Kuwabara, M., Kakinuma, Y., Ando, M., Katare, R.G., Yamasaki, F., Doi, Y., and Sato, T. (2006). Nitric oxide stimulates vascular endothelial growth factor production in cardiomyocytes involved in angiogenesis. *J Physiol Sci.* 56, 95-101.
17. Diatchenko, L., Lau, Y.F.C., Campbell, A.P., Chenchik, A., Moqadam, F., Huang, B., Lukyanov, S., Lukyanov, K., Gurskaya, N., Sverdlov, E.D., and Siebert, P.D. (1996). Suppression subtractive hybridization: a method for generating differentially regulated or tissue-specific cDNA probes and libraries. *Proc Natl Acad Sci USA.* 93, 6025-6030.
18. Choi, Y.S., Lee, H.K., and Pak, Y.K. (2002). Characterization of the 5'-flanking region of the rat gene for mitochondrial transcription factor A (Tfam). Biochim Biophys Acta. 1574, 200-204.
19. Wang, L., Ma, W., Markovich, R., Chen, J.W., and Wang, P.H. (1998). Regulation of cardiomyocyte apoptotic signaling by insulin-like growth factor I. *Circ Res.* 83, 516–522.
20. Gurtu, V., Kain, S.R., and Zhang, G. (1997). Fluorometric and colorimetric detection of caspase activity associated with apoptosis. *Anal Biochem* 251, 98-102.
21. Larsson, N.G., Wang, J., Wilhelmsson, H., Oldfors, A., Rustin, P., Lewandoski, M., Barsh, G.S., and Clayton, D.A. (1998). Mitochondrial transcription factor A is necessary for mtDNA maintenance and embryogenesis in mice. *Nat Genet.* 18, 231-236.
22. Wang, J., Wilhelmsson, H., Graff, C., Li, H., Oldfors, A., Rustin, P., Bruning, J.C., Kahn, C.R., Clayton, D.A., Barsh, G.S., Thoren, P., Larsson, N.G. (1999). Dilated cardiomyopathy and atrioventricular conduction blocks induced by heart-specific inactivation of mitochondrial DNA gene expression. *Nat Genet.* 21:133-137.

23. Tewari, M., Yu, M., Ross, B., Dean, C., Giordano, A., and Rubin, R. (1997). AAC-11, a novel cDNA that inhibits apoptosis after growth factor withdrawal. *Cancer Res.* 57, 4063-4069.
24. Sasaki, H., Moriyama, S., Yukiue, H., Kobayashi, Y., Nakashima, Y., Kaji, M., Fukai, I., Kiriyama, M., Yamakawa, Y., and Fujii, Y. (2001). Expression of the antiapoptosis gene, AAC-11, as a prognosis marker in non-small cell lung cancer. *Lung Cancer* 34, 53-57.
25. Kim, J.W., Cho, H.S., Kim, J.H., Hur, S.Y., Kim, T.E., Lee, J.M., Kim, I.K., and Namkoong, S.E. (2000). AAC-11 overexpression induces invasion and protects cervical cancer cells from apoptosis. *Lab Invest.* 80, 587-594.
26. Duchen, M.R. (2004). Roles of mitochondria in health and disease. *Diabetes* 53 Suppl 1, S96-102.
27. Saelens, X., Festjens, N., Vande Walle, L., van Gurp, M., van Loo, G., and Vandenabeele P. (2004). Toxic proteins released from mitochondria in cell death. *Oncogene* 23, 2861-2874.
28. Herbert, L.J. (1997). Rest heart rate and life expectancy. *J Am Coll Cardiol.* 30, 1104-1106.
29. Sohal, R.S., and Weindruch, R. (1996). Oxidative stress, caloric restriction, and aging. *Science* 273, 59-63.
30. Ruffolo, R.R. Jr, and Feuerstein, G.Z. (1997). Pharmacology of carvedilol: rationale for use in hypertension, coronary artery disease, and congestive heart failure. *Cardiovasc Drugs Ther.* 11 Suppl 1, 247-256.
31. Chandel, N.S., Maltepe, E., Goldwasser, E., Mathieu, C.E., Simon, M.C., and Schumacker, P.T. (1998). Mitochondrial reactive oxygen species trigger hypoxia-induced transcription. *Proc Natl Acad Sci U S A.* 95, 11715-11720.
32. Fleury, C., Mignotte, B., and Vayssiere, J.L. (2002). Mitochondrial reactive oxygen species in cell death signaling. *Biochimie* 84, 131-141.
33. Thuerauf, D.J., Marcinko, M., Gude, N., Rubio, M., Sussman, M.A., and Glembotski, C.C. (2006). Activation of the unfolded protein response in infarcted mouse heart and hypoxic cultured cardiac myocytes. *Circ Res.* 99, 275-282.
34. Terai, K., Hiramoto, Y., Masaki, M., Sugiyama, S., Kuroda, T., Hori, M., Kawase, I., and Hirota, H. (2005). AMP-activated protein kinase protects cardiomyocytes against hypoxic injury through attenuation of endoplasmic reticulum stress. *Mol Cell Biol.* 25, 9554-9575.
35. Kanazawa, A., Nishio, Y., Kashiwagi, A., Inagaki, H., Kikkawa, R., and Horiike, K. (2002). Reduced activity of mtTFA decreases the transcription in mitochondria

isolated from diabetic rat heart. *Am J Physiol Endocrinol Metab.* 282, E778-785.

Figure legends

Figure 1

The protein level of HIF-1α is greatly increased in VHL-negative cells compared with VHL-positive cells, even under normoxia.

VHL-positive cells express the VHL protein, whereas VHL-negative cells do not. By contrast, VHL-negative cells express more HIF-1α protein, even under normoxia, than VHL-positive cells (n=4). Representative data are shown.

Figure 2

VHL-negative cells show lower expression of GRP78 protein with reduced mitochondrial function.

A, both VHL-positive cells and VHL-negative cells proliferate well without cell death, as evaluated by the absence of floating cells. When the numbers of both cell types are comparable, evaluated by counting cells, no morphological differences are observed. B, VHL-negative cells show lower GRP78 expression than VHL-positive cells despite the comparable cell numbers, as indicated by the α-tubulin expression levels (n=4). C, compatible with decreased GRP78 expression, VHL-negative cells also show significantly lower MTT reduction activity (74.6±5.3%) than VHL-positive cells (100.0±3.7%; n=6, $P<0.01$), despite the comparable cell numbers.

Figure 3

The expression of the AI gene, which is localized in the nucleus, is increased under hypoxia and involved in the reduction of GRP78 expression through HIF-1α.

A, even under normoxia, AI mRNA gene expression is increased in VHL-negative cells compared with VHL-positive cells, as evaluated by RT-PCR (n=5). B, AI mRNA expression is increased by hypoxia (1% oxygen) in HEK293 cells as well as H9c2 cells (n=5). C, The wild-type form (WT) of HIF-1α slightly increases AI gene expression; however, the dominant negative form (DN) adversely decreases AI gene expression, as evaluated by RT-PCR (n=6, $P<0.01$). D, Compared with WT HIF-1α, GRP78 expression was up-regulated by DN HIF-1α (n=3, $P<0.05$). E, AI suppresses the increase in GRP78 expression in HEK293 cells induced by 5 μg/ml tunicamycin; adversely non-transfected control cells, GFP-transfected cells and empty vector-transfected cells all responded to tunicamycin with elevated GRP78 expression (n=5). F, labeling with an anti-His tag antibody reveals that the His-tagged AI protein is localized in the nucleus, and not in the cytoplasm.

Figure 4

The AI gene regulates mitochondrial function by modifying the transcriptional activation of mitochondrial transcription factor A (TFAM), leading to a decrease in oxygen consumption, and inhibition of hypoxia-induced apoptosis.

A, the MTT reduction activity in AI-transfected cells is decreased (to 43.0±2.5%) compared with that in GFP-transfected cells (101.3±3.1%; n=8, $P<0.01$), despite the comparable cell numbers. B, reporter assays reveal that AI suppresses the transcriptional activity of TFAM in two different luciferase vectors, compared with TFAM alone (378±15 to 267±10 RLU in basic vector, 739±55 to 397±19 RLU in SV promoter vector, n=8 in each reporter assay experiment, $P<0.01$ vs. TFAM). C, The calcium response is reduced by AI. Intracellular calcium accumulation in HEK293 cells is increased in response to exogenous application of 100 μM ACh. However, in AI-transfected HEK293 cells the response is suppressed (n=20, $P<0.05$ vs. GFP). Four representative calcium response traces are shown. D, Transient transfection of the AI gene into HEK293 cells decreases their oxygen consumption compared with that in GFP-transfected cells, as evaluated by the RCI. Furthermore, rat primary cardiomyocytes infected with AI adenovirus also show reduced oxygen consumption (n=5, $P<0.05$ vs. GFP or LacZ). E, caspase-3 activity in HEK293 cells is increased by hypoxia, and AI suppresses this elevation of caspase-3 activity (n=5, $P<0.01$ vs. control). F, knockdown of the AI gene significantly increases the MTT reduction activity in HEK293 cells under ordinary culture conditions, compared with that of non-transfected control cells or unrelated siRNA-transfected cells (n=10, $p<0.01$ vs. control or unrelated siRNA). G, Myocardial ischemia for 3 hours increased the level of AI mRNA expression in the heart, compared with non-ischemic heart, as evaluated by RT-PCR (n=4).

Kakinuma
Figure 1

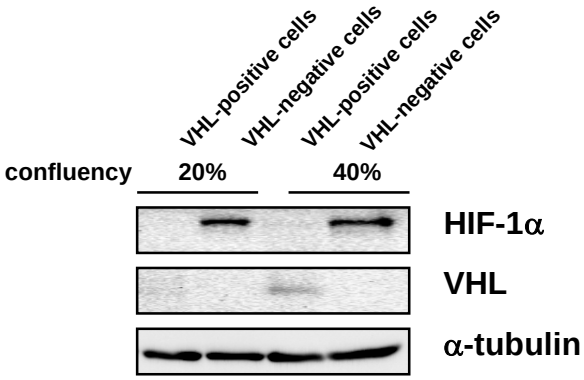

Figure 2

A

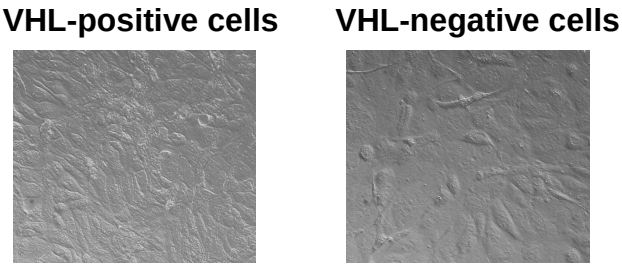

B

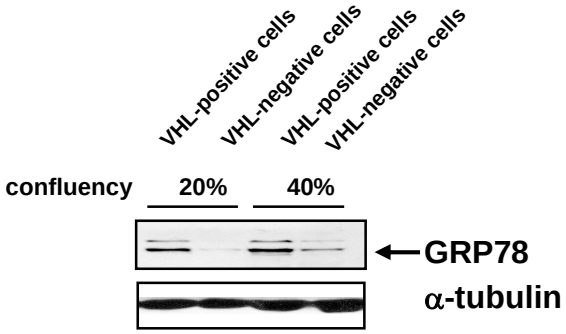

C

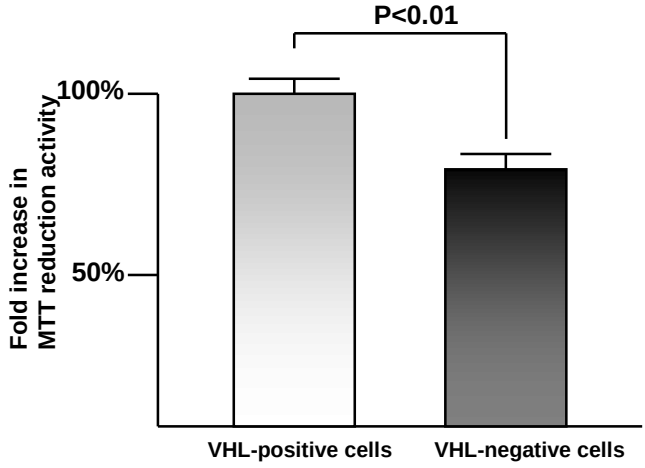

Kakinuma
Figure 3

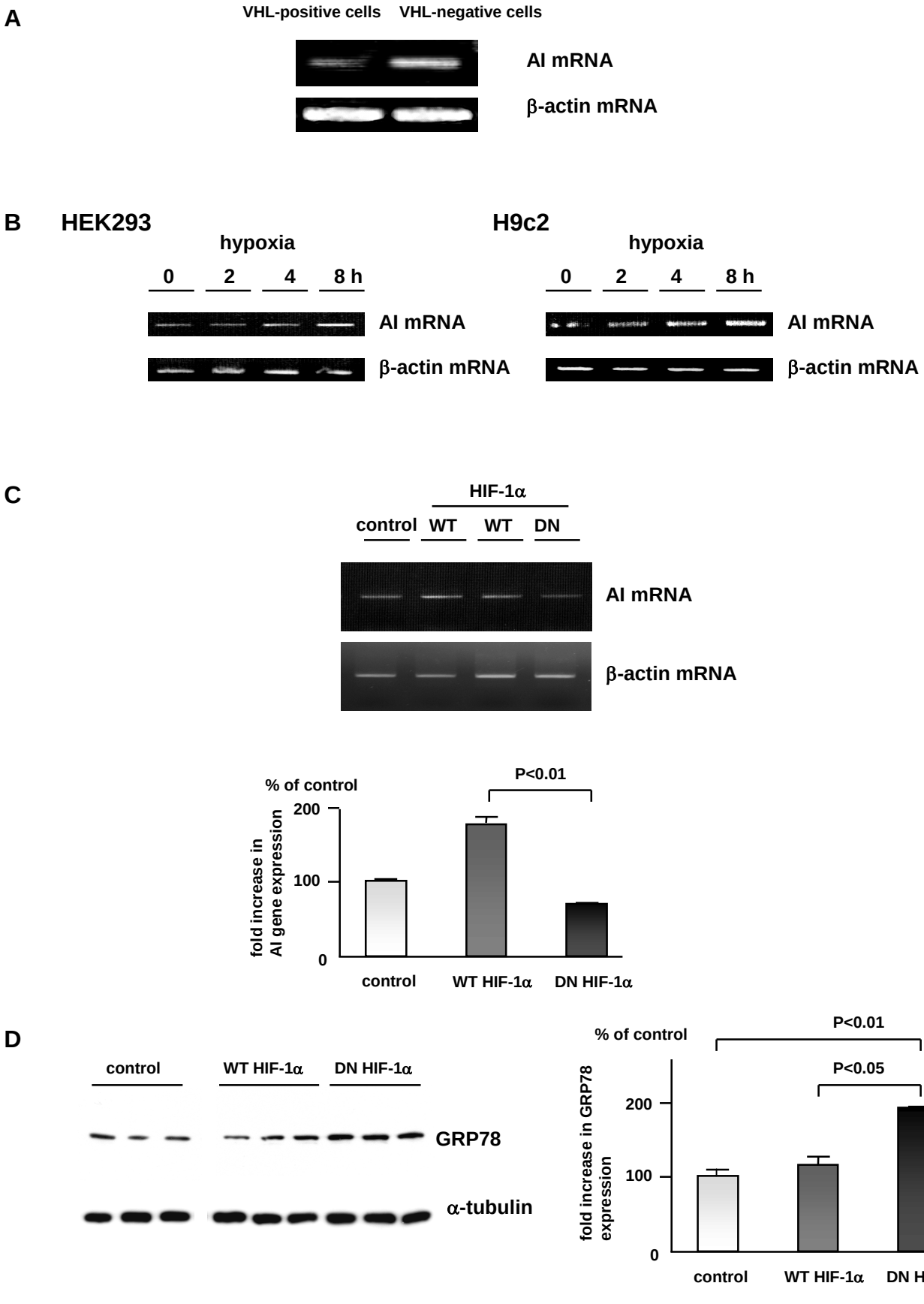

Kakinuma
Figure 3

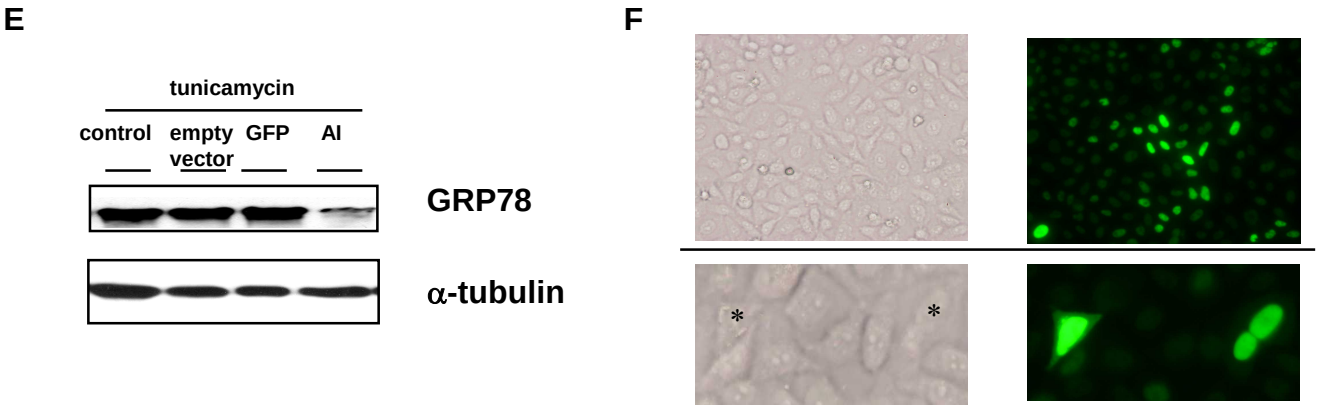

Figure 4

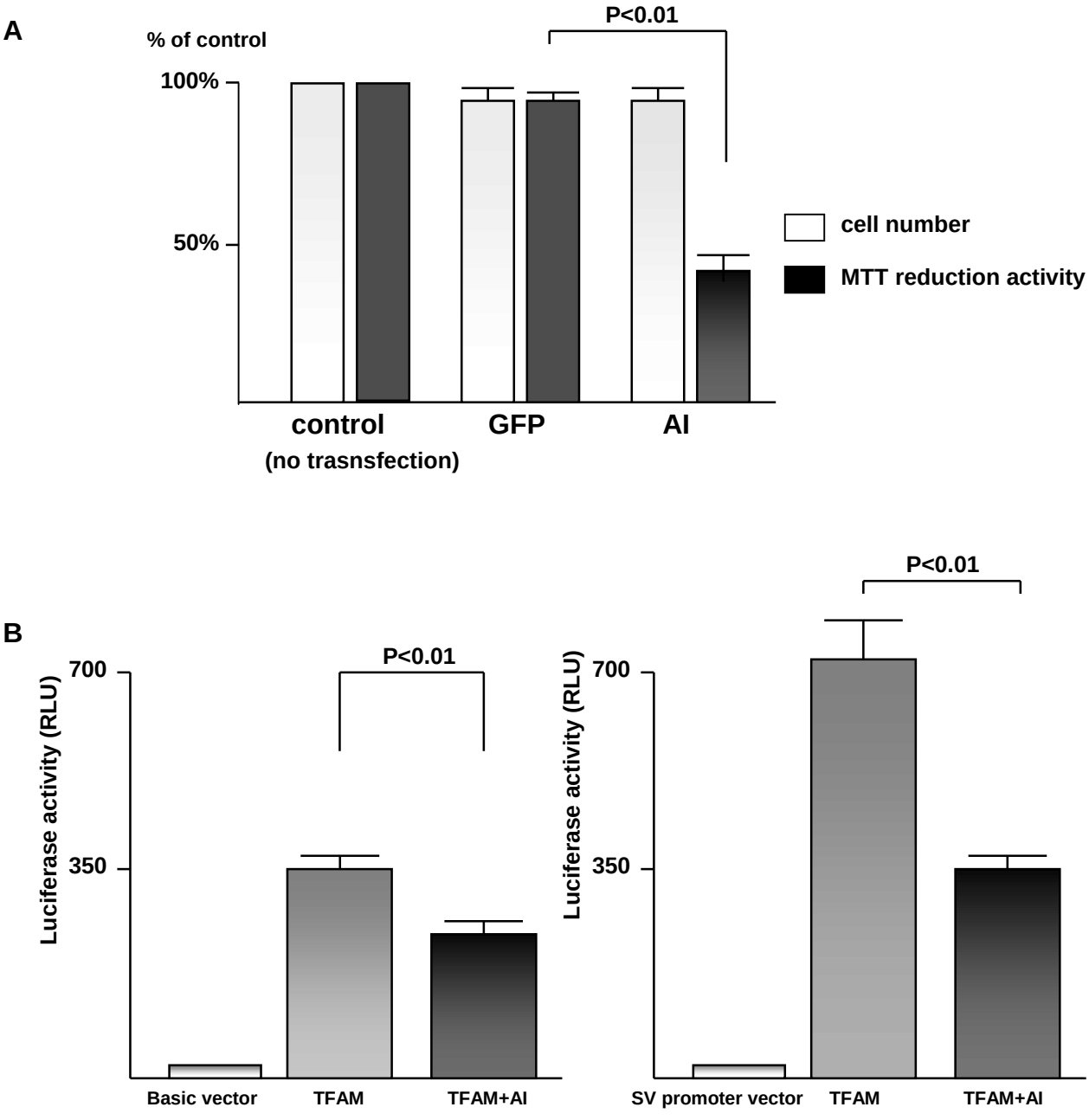

Kakinuma
Figure 4

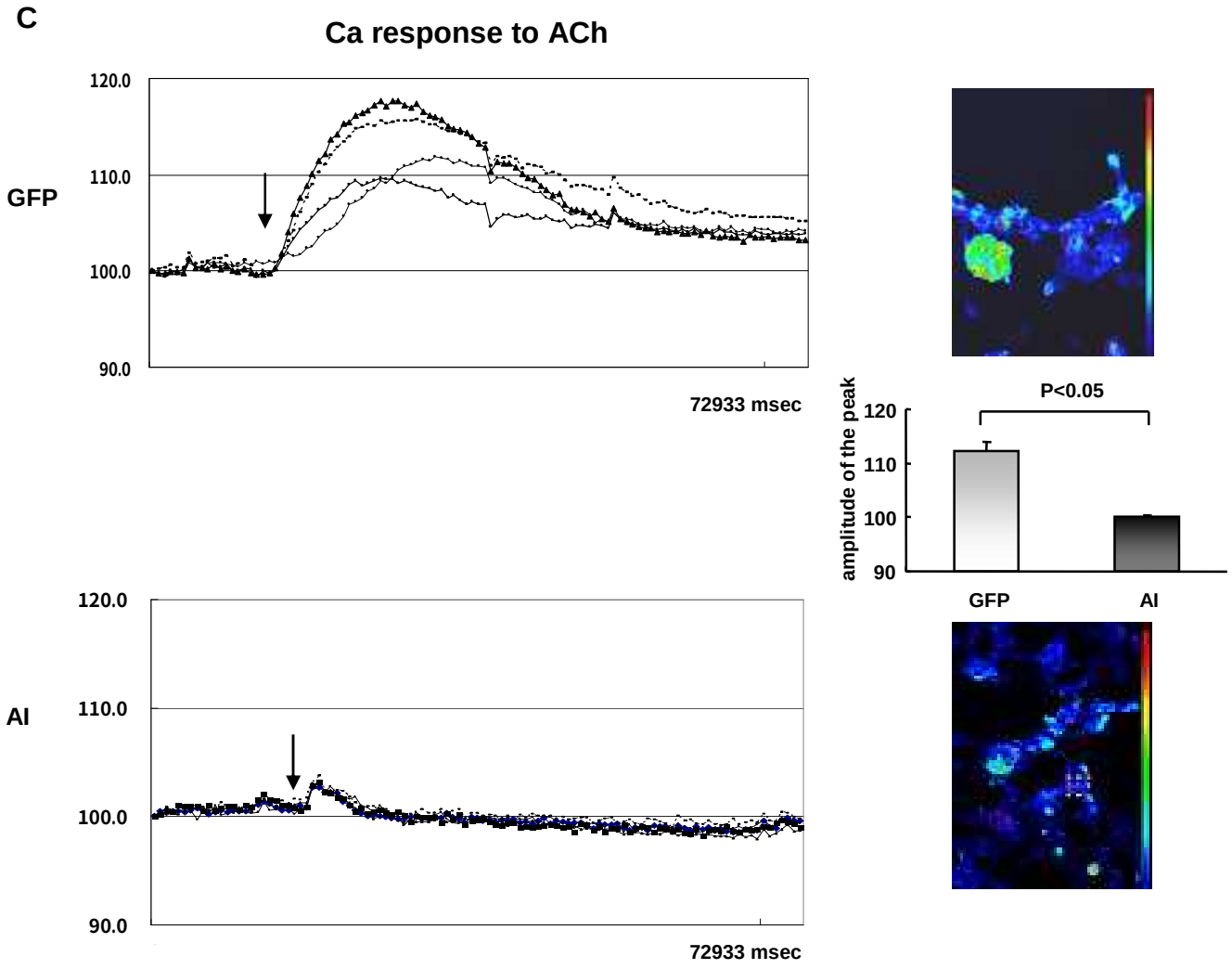

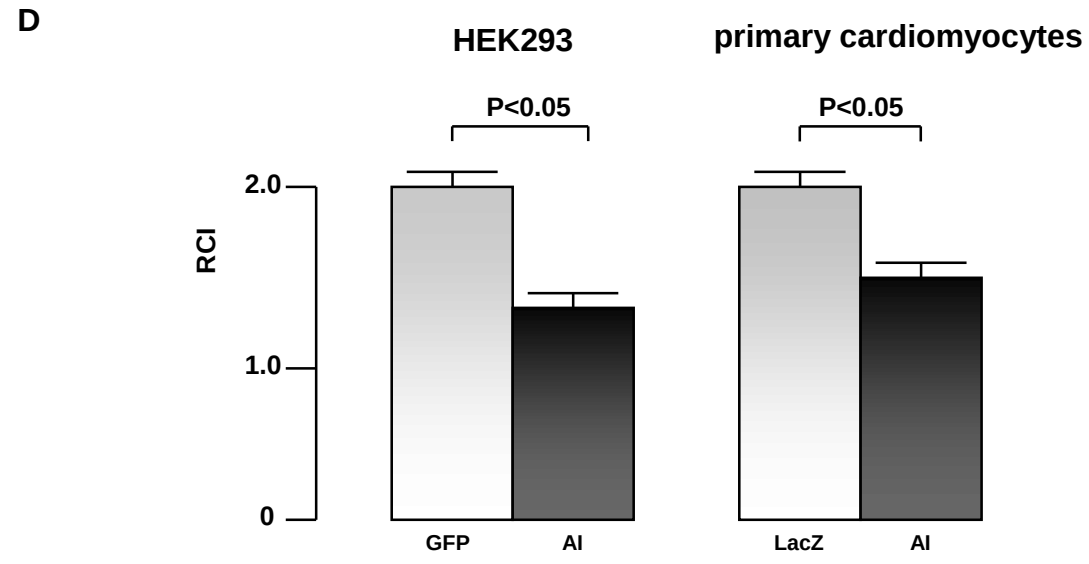

Kakinuma
Figure 4

E

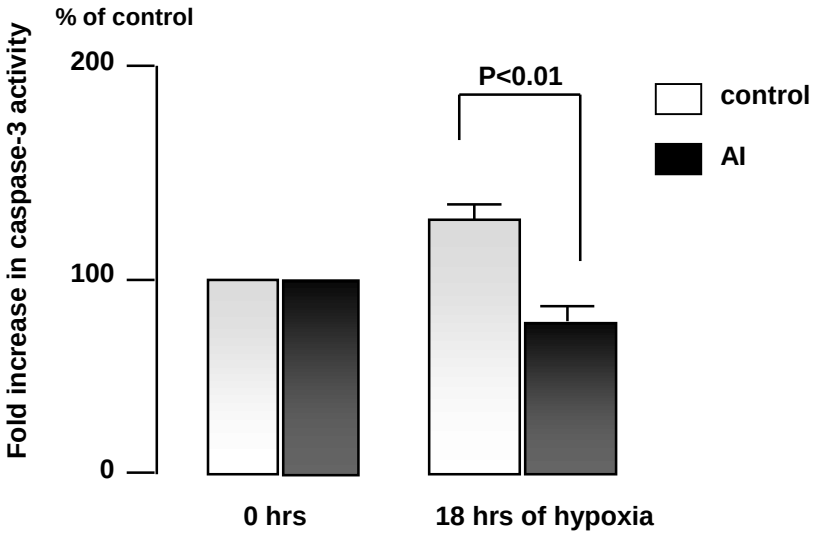

F

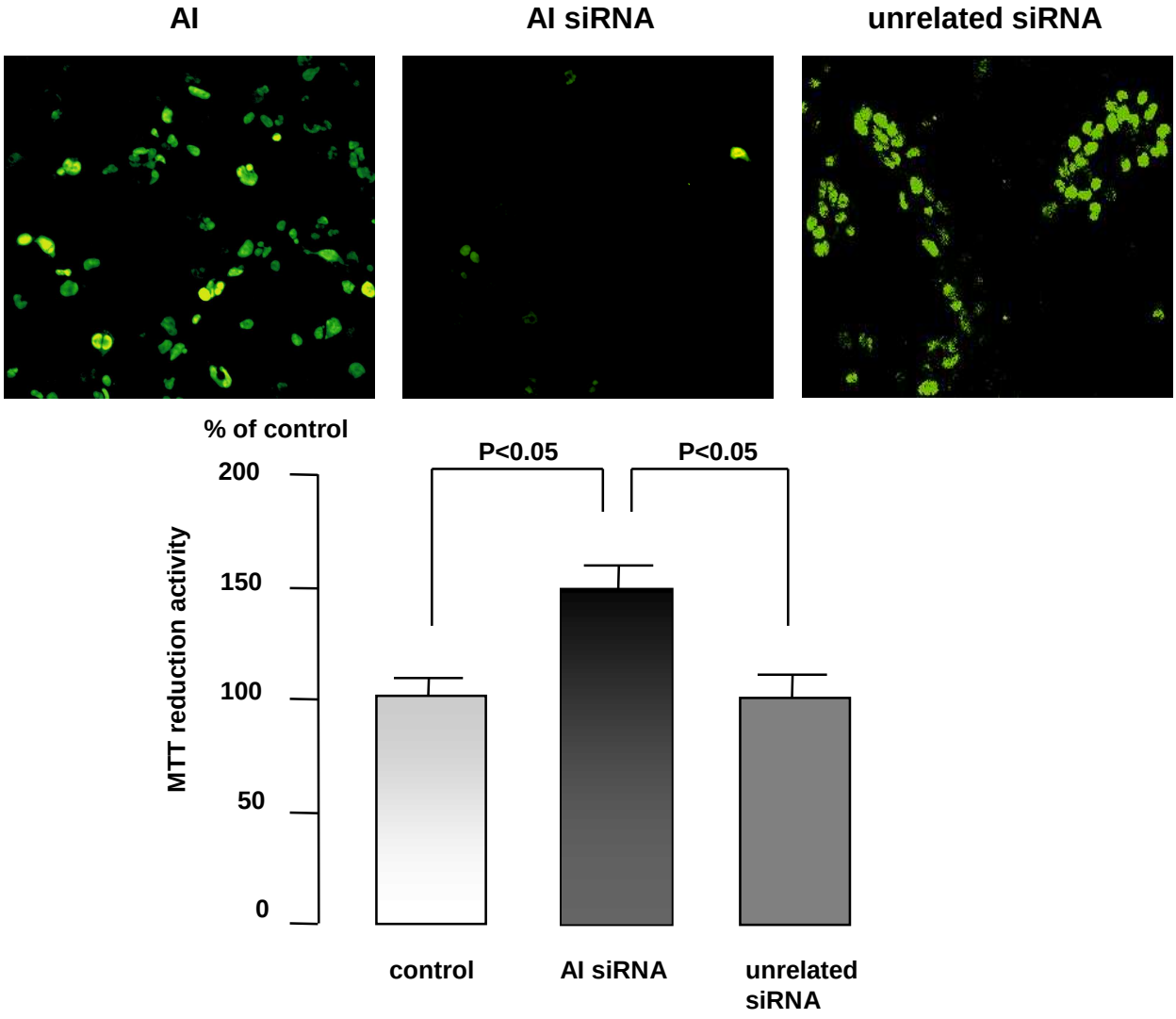

G